GZMA and *RASGRP1* are novel tumor suppressors that counter dissemination of *Theileria annulata*-transformed macrophages

Zineb Rchiad[1,2,3*], Malak Haidar[1,2,3*], Hifzur Rahman Ansari[3,4°], Shahin Tajeri[1,2°], Fathia Ben Rached[3], Gordon Langsley[1,2#], Arnab Pain[3,5#]

[1]Inserm U1016, Cnrs UMR8104, Cochin Institute, Paris, 75014 France.
[2]Laboratoire de Biologie Cellulaire Comparative des Apicomplexes, Faculté de Médecine, Université Paris Descartes - Sorbonne Paris Cité, France.
[3]Pathogen Genomics Laboratory, BESE Division, King Abdullah University of Science and Technology (KAUST), Thuwal-23955-6900, Kingdom of Saudi Arabia.
[4]King Abdullah International Medical Research Center (KAIMRC), King Abdulaziz Medical City, Ministry of National Guard Health Affairs, Jeddah 21423, Saudi Arabia.
[5]Global Station for Zoonosis Control, Global Institution for Collaborative Research and Education (GI-CoRE), Hokkaido University, N20 W10 Kita-ku, Sapporo, Japan.

*Co-first authors; °Co-second authors
#Corresponding authors:
Gordon Langsley; Email: gordon.langsley@inserm.fr
Arnab Pain; Email: arnab.pain@kaust.edu.sa

Running Title: Role of Key Genes in *Theileria annulata*-mediated Leukocyte Transformation

Key Words: *Theileria annulata*, Transformation; Transcriptome; Dissemination; *RASGRP1*; *GZMA;* Tumor suppressor

Financial Support: This study was supported by the Competitive Research Grant 4 (OSR-2015-CRG4-2610) from the Office for Sponsored Research in King Abdullah University of Science and Technology (KAUST). ST was supported by a ParaFrap post-doctoral fellowship and GL acknowledges support from Labex ParaFrap (ANR-11-LABX-0024), INSERM and the CNRS.

Abstract

Theileria annulata is a tick-transmitted apicomplexan parasite that infects and transforms bovine leukocytes into disseminating tumors that cause a disease called tropical theileriosis. Using RNA sequencing we identified bovine genes, whose transcription is perturbed during *Theileria*-induced transformation to define the transcriptional atlas of transformed virulent versus attenuated (dampened dissemination) macrophages and transformed B cells. Dataset comparisons highlighted a small set of novel genes associated with *Theileria*-transformed leukocyte dissemination and the roles of Granzyme A (*GZMA*) and RAS guanyl-releasing protein 1 (*RASGRP1*) confirmed by CRISPR/Cas9-mediated down-regulation of their expression. Knockdown of both *GZMA* and *RASGRP1* in attenuated macrophages led to a regain in their dissemination in Rag2/γC mice confirming *in vivo* both *GZMA* and *RASGRP1* as novel dissemination suppressors.

INTRODUCTION

Theileria annulata is a tick-transmitted apicomplexan parasite that infects and transforms bovine leukocytes into disseminating tumors that cause a widespread disease called tropical theileriosis. In countries endemic for tropical theileriosis live attenuated vaccines are produced by long-term passage of virulent, transformed macrophages that following multiple passages (circa 300) in the laboratory loose the lethal disseminating phenotype, thus allowing them to vaccinate and transiently protect animals against disease (1). Amazingly the fully transformed state can be completely reversed by drug-induced parasite death making *Theileria*-infected leukocytes a powerful cellular model to identify genes regulating cellular transformation (2). This parasite-based reversible model of leukocyte transformation has been exploited to show how a secreted peptidyl-prolyl isomerase (PIN1) by interacting with the ubiquitin ligase FBW7 stabilizes c-Jun (3), how SMYD3 is a key regulator of *MMP*-9 transcription (4), and how c-Jun NH2-terminal kinase/c-Jun signaling promotes survival and dissemination of B cells transformed by *Theileria* (5). In addition to being reversible, loss of dissemination of live attenuated vaccines offers the opportunity to search for novel regulators of tumor dissemination, rather than survival and immortalization. For example, we exploited the Ode *T. annulata* attenuated vaccine to highlight the role that TGF-β2 (transforming growth factor) plays in dissemination, since exogenous TGF-β2-stimulation of attenuated macrophages led to a regain in the virulent dissemination phenotype (6). In virulent macrophages high levels of secreted TGF-β2 induce Grb2 to recruit PI3-K to TGF-RII activating JNK/AP-1-signaling and promoting tumor dissemination (7). By contrast, in attenuated macrophages loss of TGF-β2 production ablates expression of COX2 and EP4 leading to a drop in cyclic AMP (cAMP) levels and reduced activation of protein kinase A (PKA) and EPAC (8).

Epigenetics also contributes to *Theileria*-induced leukocyte transformation (9). OncomiR addiction has been described as being generated by a miR-155 feedback loop in *T. annulata*-transformed B cells (10). RNA from transformed B cells was used to screen a miRNA microarray and 6 miRs were found to be downregulated upon drug-induced parasite death including miR-155. Infection-induced miR-155 ablated DET leading to stabilization of c-Jun to drive expression of BIC transcripts harboring miR-155 (10). Specific deep RNA-seq generated miRomes for non-infected B cells, *T. annulata*-transformed B cells and virulent and attenuated macrophages (11). The logic being that *Theileria*-induced macrophage transformation activated oncogenes and ablated tumor suppressors, while in attenuated, non-disseminating macrophages, oncogene transcription is ablated and tumor suppressor expression increased. miR-126-5p was identified by these criteria, since its infection-induced upregulation suppressed JNK-Interacting Protein (JIP) liberating JNK to translocate to the nucleus and phosphorylate c-Jun, and miR-126-5p loss in attenuated macrophages led to a regain in JIP expression that retained JNK1 in the cytosol so dampening c-Jun phosphorylation and hence *mmp9* transcription (11). Therefore, changes in miR-126-5p levels contribute to both virulent hyper-dissemination and attenuated dissemination of *T. annulata*-transformed macrophages.

RNA extracted from *T. annulata*-transformed B cells was used to screen bovine microarrays and infection reconfigured B cell gene expression (12). As *Theileria*-induced transformation constitutively activates transcription factors such as NF-κB, c-Myc and AP-1, reviewed in (13, 14) alterations in gene expression identified some of the pathways related leukocyte transformation (15). Nonetheless, a systematic and genome scale transcriptional comparison of B cells and macrophages transformed *T. annulata* has been lacking. With the availability of next generation sequencing technologies (RNA-seq), it is

possible to obtain an unbiased and comprehensive catalogue of gene expression and an understanding of their perturbations due to *T. annaulata*-mediated leukocyte transformation. In this study, RNA-seq was used to define the transcriptional landscapes of two *T. annulata*-transformed B-cell lines and the virulent *T. annulata*-transformed macrophage line as well as the Ode attenuated live vaccine directly derived from it. Bioinformatic comparisons of the transcriptional landscapes at high stringency identified four candidate genes as potential players in the dissemination of virulent *T. annulata*-transformed macrophages. We provide functional evidence that both *GZMA* and *RAGRP1* are novel suppressors of tumor dissemination.

Materials and Methods

Cell lines

The BL3 (16), TBL3, BL20 (17), TBL20 (18) B lymphocytes and Ode macrophages (19) were cultured in RPMI 1640 medium supplemented with 2 mM of L-glutamine (Lonza, catalogue number 12-702F) and 10 mM Hepes (Lonza, catalogue number 17-737E), 10 % heat-inactivated FBS (Gibco, catalogue number 10082147), 100 units/ml of Penicillin and 100 ug/ml of streptomycin (Lonza, catalogue number 17-602E) and 10mM b-mercaptoethanol (Sigma-Aldrich, catalogue number M6250) for BL3/TBL3 and BL20/TBL20. The virulent (Vir) hyper-disseminating Ode cell line was used at low passage (53-71), while its attenuated (Att) poorly disseminating vaccine counterpart corresponded to passages 309-317. All cell lines were incubated at 37°C with 5% CO_2.

RNA extraction

Cells were seeded in 3 biological replicates at a density of $2.5x10^5$ cell/ml. RNA extraction was performed using the PureLink RNA Mini Kit (Life technologies, catalogue number 12183018A) following the manufacturer's instructions. Briefly, cells were pelleted, lysed and homogenized using a 21-gauge needle, then 70% ethanol was added to the cell lysates and the samples were loaded on spin cartridges to bind RNA. After 3 washes, RNA was eluted in RNase-free water. The quality of extracted RNA was verified using a Bioanalyzer 2100 and quantification carried using Qubit (Invitrogen, catalogue number Q10210).

Library preparation and sequencing

Strand-specific RNA-sequencing (ssRNA-seq) libraries were prepared using the illumina Truseq Stranded mRNA Sample Preparation Kit (illumina, catalogue number RS-122-2101) following the manufacturer's instructions. Briefly, 1ug of total RNA was used to purify mRNA using poly-T oligo-attached magnetic beads. mRNA was then fragmented

and cDNA was synthesized using SuperScript III reverse transcriptase (Thermofisher, catalogue number 18080044), followed by adenylation on the 3' end, barcoding and adapter ligation. The adapter ligated cDNA fragments were then enriched and cleaned with Agencourt Ampure XP beads (Agencourt, catalogue number A63880). Libraries validation was conducted using the 1000 DNA kit on 2100 Bioanalyzer (Agilent Technologies, catalogue number 5067-1504) and quantified using qubit (Thermofisher, catalogue number Q32850). ssRNA libraries were sequenced on Illumina Hiseq2000. The sequenced reads were mapped to the *Bos taurus* genome Btau 4.6.1. The quality of the sequenced libraries is shown in supplementary figure S1.

Sequencing data analysis

The quality of sequence reads and other parameters were checked using FastQC (http://www.bioinformatics.babraham.ac.uk/projects/fastqc/). The raw RNA-seq reads were processed for adaptor trimming by Trimmomatic (20). The strand-specific reads were mapped on to Bovine genome (bosTau7; Btau_4.6.1; GCF_000003205.5) using Tophat2 (-g 1 --library-type fr-firststrand) (21). The samples with respective replicates were analyzed further for differential gene expression by three different tools, baySeq (22), DESeq2 (fitType ="local") (23) and CuffDiff2 (24) with default parameters unless mentioned specifically. The count values for DESeq2 and baySeq were calculated from BAM files using HTSeq-count tool (25). The transcriptome quality plots were generated by cummeRbund package (v2.14.0) in R (http://bioconductor.org/packages/release/bioc/html/cummeRbund.html).

Identification of differentially expressed genes after infection and attenuation by comparative transcriptome analysis

The transcriptome data was analyzed with baySeq (22), DESeq2 (23) and CuffDiff2 (24). A gene was considered as a differentially expressed gene (DEG) if it has a padj<0.05 and a fold change (FC)>2. The final list of DEGs contained genes commonly differentially

expressed in CuffDiff2, DESeq2 and baySeq. This approach minimalizes the total number of DEGs for further analysis and allows stringent selection of the most significant and reproducible DEGs.

qRT-PCR

Total RNA was reverse transcribed using the High Capacity cDNA Reverse Transcription Kit (Applied biosystems, catalogue number 4368814) as follows: 2 μg of total RNA, 2 μL of RT buffer, 0.8 μL of 100mM dNTP mix, 2.0 μL of 10X random primers, 1 μL of MultiScribe reverse transcriptase and Nuclease-free water to a final volume of 20 μL. The reaction was incubated 10 min at 25°C, 2 h at 37°C then the enzyme inactivated at 85°C for 5 min. Real time PCR was performed in a 10 μL reaction containing 20-30 ng cDNA template, 5 μL 2X Fast SYBR Green Master Mix and 500 nM of forward and reverse primers. The reaction was run on the 7500 HT Fast Real-Time PCR System (Applied Biosystems). GAPDH was used as a housekeeping gene and the results were analyzed by the $2^{-\Delta\Delta CT}$ method (26). The error bars represent the SEM of 3 biological replicates. Primers were designed and assessed for secondary structures using the Primer Express Software v3.0. The primers of all genes are listed in Table S3.

Transfection

Macrophages were transfected by electroporation using the Nucleofector system (Amaxa Biosystems). A total of 5 × 10^5 cells were suspended in 100 μl of Nucleofector V solution mix (Lonza, VCA-1003) with 2 μg of *GZMA* and *RASGRP1* CRISPR/Cas9 plasmids and subjected to electroporation using the cell line-specific program T-O17. After transfection, cells were suspended in fresh complete medium and incubated at 37°C with 5% CO_2 for 24 to 48 h.

Western blotting

Cells were harvested and extracted by RIPA lysis buffer supplemented with the PhosSTOP phosphatase inhibitor cocktail tablets (Roche, catalogue number 04906845001) and Complete mini EDTA free protease inhibitor cocktail tablets (Roche, catalogue number 05 892 970 001). Protein concentration was determined by the Bradford protein assay. Cell lysates were subjected to Western blot analysis using conventional SDS/PAGE and protein transfer to nitrocellulose filters (Protran, Whatman, catalogue number GE10600006). The membrane was blocked by 5% non-fat milk-TBST for 2 h at room temperature. Antibodies used in immunoblotting were as follows: mouse monoclonal antibody anti-GZMA1 (Santa Cruz Biotechnologies, catalogue number sc-33692) and rabbit polyclonal antibody anti-GAPDH (Merck Millipore, catalogue number ABS16). After washing, proteins were visualized with ECL western blotting detection reagents (Thermo Scientific, catalogue number 32106) on X-ray films. The GAPDH level was used as a loading control throughout all experiments.

Matrigel chamber assay

The invasive capacity of Ode macrophages was assessed *in vitro* using matrigel migration chambers, as described in (5). The CultureCoat Medium basement membrane extract (BME) 96-wells cell invasion assay was performed according to Culturex instructions (Trevigen, catalog number 3482-096-K). After 24 h of incubation at 37°C, each well of the top chamber was washed once in buffer. The top chamber was placed back onto the receiver plate. One hundred microliters of cell dissociation solution-Calcein AM was added to the bottom chamber of each well, and the mixtures were incubated at 37°C for 1 h with fluorescently labeled cells to dissociate the cells from the membrane before reading at 485-nm excitation and 520-nm emission wavelengths, using the same parameters as those used for the standard curve.

Soft agar colony forming assay:

A two-layer soft agar culture system was used. Cell counts were performed by ImageJ software. A total of 2,500 cells were plated in a volume of 1.5 ml (0.7% bacto Agar+2× RPMI 20% Fetal bovine Serum) over 1.5 ml base layer (1% bacto agar +2× RPMI 20% Fetal bovine Serum) in 6-well plates. Cultures were incubated in humidified 37°C incubators with an atmosphere of 5% CO_2 in air, and control plates were monitored for growth using a microscope. At the time of maximum colony formation (10 days in culture), final colony numbers were counted after fixation with 0.005% Cristal Violet. The error bars in figure 3 represent SD values.

Intracellular levels of hydrogen peroxide (H_2O_2)

Cells were seeded at $1x10^5$ cell/well in a 96 well plate and incubated in complete medium for 18 h prior to the assay. Cells were then washed with PBS and incubated with 100 μ L of 5 M H2-DCFDA in PBS (Molecular Probes, catalogue number D399). H_2O_2 levels were assayed on a fusion spectrofluorimeter (PackardBell) by spectrofluorimetry at 485 and 530nm excitation and emission wavelengths respectively.

***In vivo* mouse studies and quantification of *Theileria annulata*-transformed macrophages load in mouse tissues**

T. annualata-infected macrophage cell lines (Virulent Ode passage 53, attenuated Ode passage 309, attenuated Ode transfected with *RASGRP1* CRISPR/Cas9 knock out plasmid and attenuated Ode transfected with *GZMA* CRISPR/Cas9 knock out plasmid) were injected into four groups of five Rag2γC immunodeficient mice (27) that were equally distributed on the basis of age and sex in each group. The injection site was disinfected with ethanol and one million cells (in 200 µl PBS) were injected under the skin after gentle shaking of the insulin syringe. The mice were kept for 3 weeks and then they were sacrificed humanely and dissected. Six internal organs including heart, lung, spleen,

mesentery, left kidney and liver were taken and stored in 500 µl PBS in Eppendorf tubes at -20°C. The tissues were subjected to genomic DNA extraction using the QIAmp DNA mini kit (Qiagen, catalogue number 51304). DNA concentrations were measured by Nanodrop™ 1000 spectrophotometer (Thermo Fischer scientific) and before each quantitative PCR reaction samples were diluted to give a DNA concentration of 0.5 ng/µl. Absolute copy numbers of a single copy *T. annulata* gene (*ama-1*, TA02980) that is representative of *T. annulata*-infected macrophage load in each tissue were estimated by the method described in (28), with some modifications. *Ama-1* was cloned into pJET 1.2/blunt cloning vector using CloneJET PCR Cloning Kit (Thermo scientific, catalogue number K1232). The cloned plasmid was amplified in DH5-Alpha cells and purified with QIAfilter™ Plasmid Maxi Kit (Qiagen, catalogue number 12243). Plasmid concentration was measured using Qubit (Thermofisher, catalogue number catalogue number Q32850). The primers for cloning were: forward 5'-GGAGCTAACTCTGACCCTTCG-3'and reverse 5'-CCAAAGTAGGCCAATACGGC-3'. Quantitative PCR primers were: forward 5'-GACCGATTTCATGGCAAAGT-3'and reverse 5'-TTGGGGTCATGATGGGTTAT-3'.

Ethics statement

The protocol (12-26) was approved by the ethics committee for animal experimentation at the University of Paris-Descartes (CEEA34.GL.03312). The university ethics committee is registered with the French National Ethics Committee for Animal Experimentation that itself is registered with the European Ethics Committee for Animal Experimentation. The right to perform the mice experiments was obtained from the French National Service for the Protection of Animal Health and satisfied the animal welfare conditions defined by laws (R214-87 to R214-122 and R215-10) and GL was responsible for all experimentation, as he holds the French National Animal Experimentation permit with the authorisation number (B-75-1249).

RESULTS

Differentially expressed bovine genes in *T. annulata*-transformed leukocytes

The infection and full transformation of BL20 and BL3 cell lines with *T. annulata* caused profound transcriptional changes, as previously reported for infected BL20 cells (12). Transcriptional changes between virulent compared to attenuated Ode macrophages are less profound, likely because the macrophages are isogenic and only appear to differ in dissemination potential (Fig. 1 a).

To identify bovine genes whose transcription is perturbed by transformation and attenuation of dissemination of *T. annulata*-transformed leukocytes we concentrated on the most differentially expressed genes (DEGs) (Fig. 1 b, Table S1). Many of these genes are annotated as being implicated in cellular proliferation and metastasis. Amongst the top five-upregulated transcripts in TBL20 is *MMP9* (matrix metallopeptidase 9), a gene highly expressed in different cancer types and linked to metastasis and angiogenesis (29). *WC1-8* is the third most up-regulated gene in TBL20 lymphocytes and has been described as being also upregulated in ovarian carcinoma cells (30). The most down-regulated transcripts in TBL20 cells include *LAIR1* (leukocyte associated immunoglobulin like receptor 1) and *VPREB* (pre-B lymphocyte 1). *LAIR1* is a strong inhibitor of natural killer cell-mediated cytotoxicity and an inhibitory receptor, which down-regulates B lymphocyte immunoglobulin and cytokine production (31). Down-regulation of *LAIR-1* was not unexpected, as its loss of expression is observed during B cell proliferation (32). *ZBTB32* (zinc finger and BTB domain containing 32), *IL21R* (interleukin 21 receptor), and *MMP9* are also among the top five up-regulated transcripts in TBL3 lymphocytes. The five most down-regulated transcripts in TBL3 cells are *KRT6C* (keratin 6C), *MATK* (megakaryocyte-associated tyrosine kinase), *IGSF9B* (immunoglobulin superfamily member 9B), *A2M* (alpha-2-macroglobulin) and *H2AFY2* (H2A histone family, member Y2). The biological functions of these genes include inhibition of cell growth and proliferation (33), repression

of DNA transcription (34) and inhibition of cell adhesion and migration (35), functions that are often dampened to allow continuous proliferation and survival of transformed cells. We confirmed by qRT-PCR differential expression of 21 randomly selected genes from the BL20/TBL20 and BL3/TBL3 RNA-seq datasets (Fig. 1 c).

Identification of key genes potentially involved in *Theileria*-mediated macrophage dissemination

The most down-regulated transcripts in attenuated Ode macrophages are *SKAP2* (src kinase associated phosphoprotein 2), a gene known to promote tumor metastasis through the regulation of podosome formation in macrophages (36) and *NRP2* that regulates tumor progression by promoting TGF-β1 signaling (37). Down-regulation of these genes correlates with decreased dissemination of attenuated macrophages, as previously we have described loss of TGF-β2 signaling as being associated with decreased dissemination (6). By contrast, the most highly up-regulated transcripts include *SEPP1* (selenoprotein P) and *PTPRT* (protein tyrosine phosphatase, receptor type T) and *PTPRT* has been previously described as a tumor suppressor gene (38, 39). Taken together the identity of the most strongly up- and down-regulated genes argues that our differential transcription screen could identify novel genes regulating transformed macrophage dissemination.

To define the genes likely playing an important role in the transformation and dissemination, we compared genes differentially expressed (DE) in TBL20, TBL3 and Attenuated Ode macrophages. We assumed that the genes most likely to play a key role in both are those inversely DE in transformation and attenuation of dissemination, i.e. upregulated after infection and down-regulated upon attenuation, and vice versa. This approach identified four genes that likely play key roles in the dissemination of *Theileria*-

transformed leukocytes (Fig. 2 a).

Figure 1

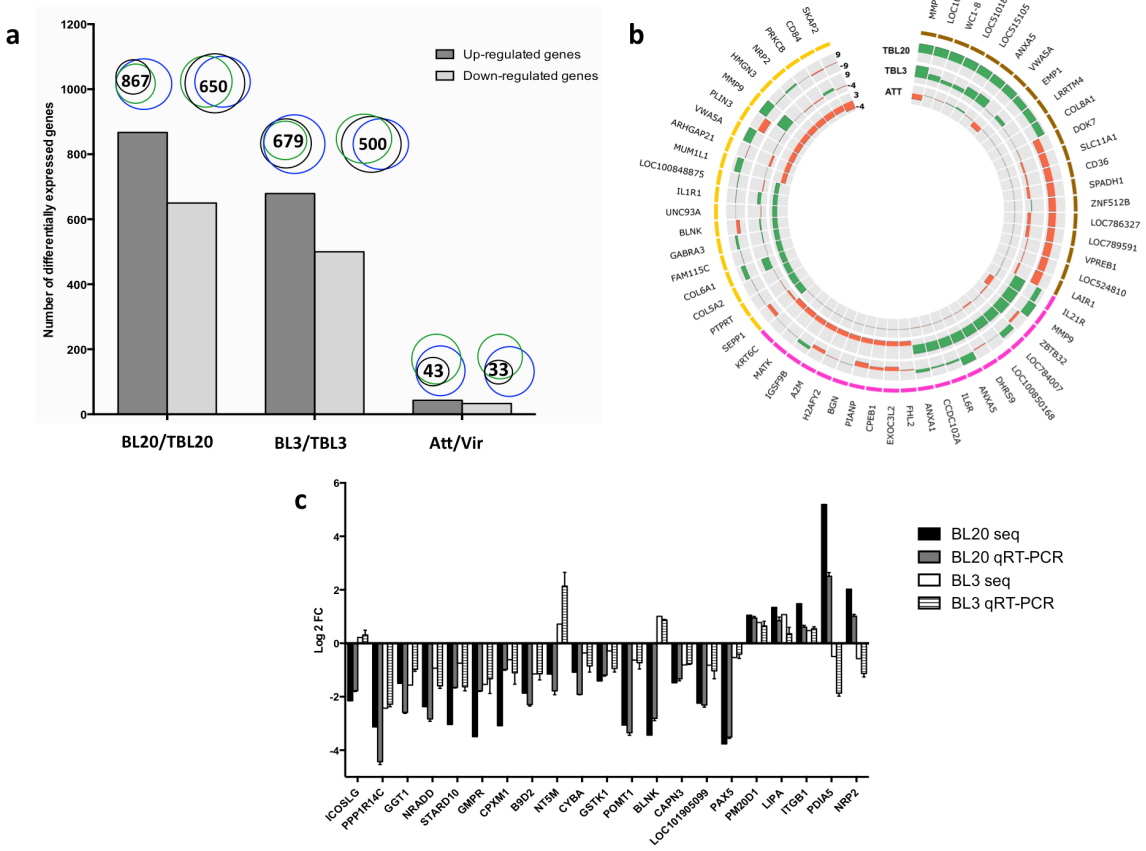

Figure 1: Differentially expressed genes in TBL20, TBL3 and Att Ode leukocytes. (a) Histogram showing the number of up- (dark grey) and down- (light grey) regulated genes in all 3 datasets. The area-proportional Venn diagrams represents the intersection between the lists of DEGs from CuffDiff2 (24) (green), DESeq2 (23) (black) and baySeq (blue) (22). The intersection between the 3 pipelines reflects the number of up- and down-regulated genes. The list of DEGs is listed in table S2. (b) Circos (40) plot showing the top 10 up- and down-regulated DEGs in BL20/TBL20 (brown), BL3/TBL3 (pink) and Att/Vir Ode (yellow). The circular heatmap represents the FC of the top DE genes in TBL20/TBL20, BL3/TBL3 and Att/Vir Ode in the outer, middle and inner rings, respectively, where green reflects the level of up-regulation and red down-regulation. (c) qRT-PCR confirmation of randomly selected genes in TBL20 and TBL3. The reactions were set in 3 biological replicates and the fold change calculating with the $2^{\Delta\Delta ct}$ method. The error bars represent SEM.

The genes are *MMP9, SEPP1, GZMA* and *RASGRP1* and their biological functions have been implicated in metastasis and cell invasion (29), selenium transport (41), peptide

cleavage by immune cells (42) and regulation of B cell-development and homeostasis and differentiation (43), respectively (Table 1). Differential expression of these genes was confirmed by qRT-PCR (Fig. 2 b). We focused on *GZMA*, *RASGRP1* and *SEPP1*, as the role of *MMP9* in metastasis/dissemination is well established including in *Theileria*-transformed macrophages (4, 44, 45). CRISPR/Cas9-mediated loss of *SEPP1* in attenuated macrophages resulted in a lethal phenotype highlighting its importance in transformed macrophage survival, rather than dissemination, and so was not characterized further.

Figure 2

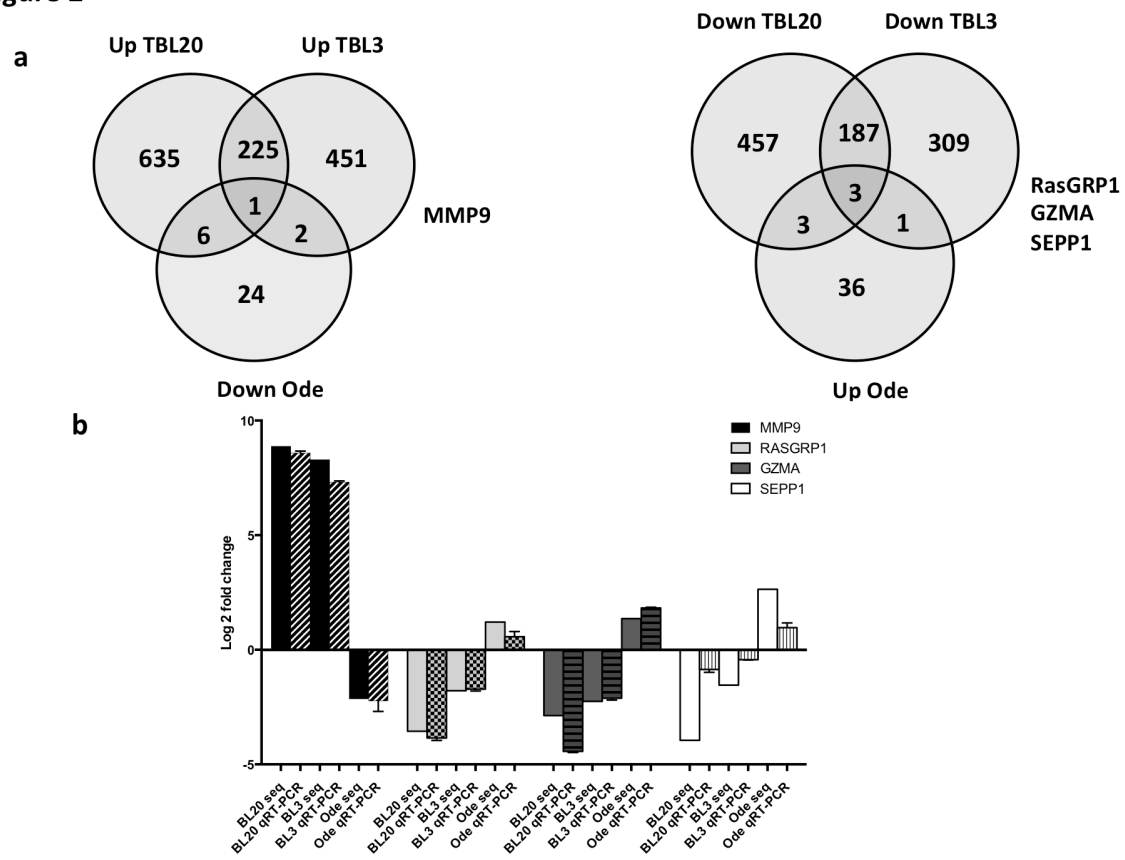

Figure 2: Inversely DEGs in TBL20, TBL3 and Att Ode leukocytes. (a) Venn diagrams illustrating the genes inversely DE in TBL20, TBL3 and Att Ode. (b) qRT-PCR confirmation of DEGs potentially playing key roles in leukocyte transformation and dissemination. The reactions were set in 3 biological replicates and the fold-change calculated with the $2^{\Delta\Delta ct}$ method. The error bars represent SEM.

Table 1: Biological functions of DEGs potentially playing key roles in leukocyte transformation and dissemination

Gene symbol	Log2 FC (TBL20)	Adj p value	Log2 FC (TBL3)	Adj p value	Log2 FC (ATT)	Adj p value	Biological functions	Reference
MMP9	8.87	0	8.29	0	-2.13	5.14 E-94	Metastasis formation, cancer cells invasion	(29)
SEPP1	-3.95	8.74 E-174	-1.54	3.75 E-248	2.63	1.01 E-140	Transports selenoprotein. Tumor suppressor	(46), (47)
GZMA	-2.87	1.45 E-05	-2.25	1.97 E-41	1.02	9.14 E-21	Plays a role in killing pathogen infected cells and cancer cells	(42)
RASGRP1	-3.55	0	-1.78	1.97 E-41	1.2	2.15 E-15	Required for correct functioning of lymphocytes in chronic infections	(43)

Ablation of GZMA and RASGRP1 by CRISPR/Cas9 knockdown

To gain insight into the implication of *GZMA* and *RASGRP1* in dissemination of *T. annulata*-transformed Ode macrophages, we knocked down their expression by CRISPR/Cas9 and confirmed that this led to decreased mRNA expression before testing poorly disseminating attenuated macrophages for a regain in dissemination phenotype in matrigel traversal assays (Fig. 3b). This indicated that GZMA and RASGRP1 have the potential to function as suppressors of tumor dissemination. Knockdown of *RASGRP1* also led to a regain in the ability of attenuated macrophages to form colonies in soft agar (Fig.3c). Taken together it indicates that GZMA and RASGRP1 have the potential to function as tumor suppressors.

Figure 3

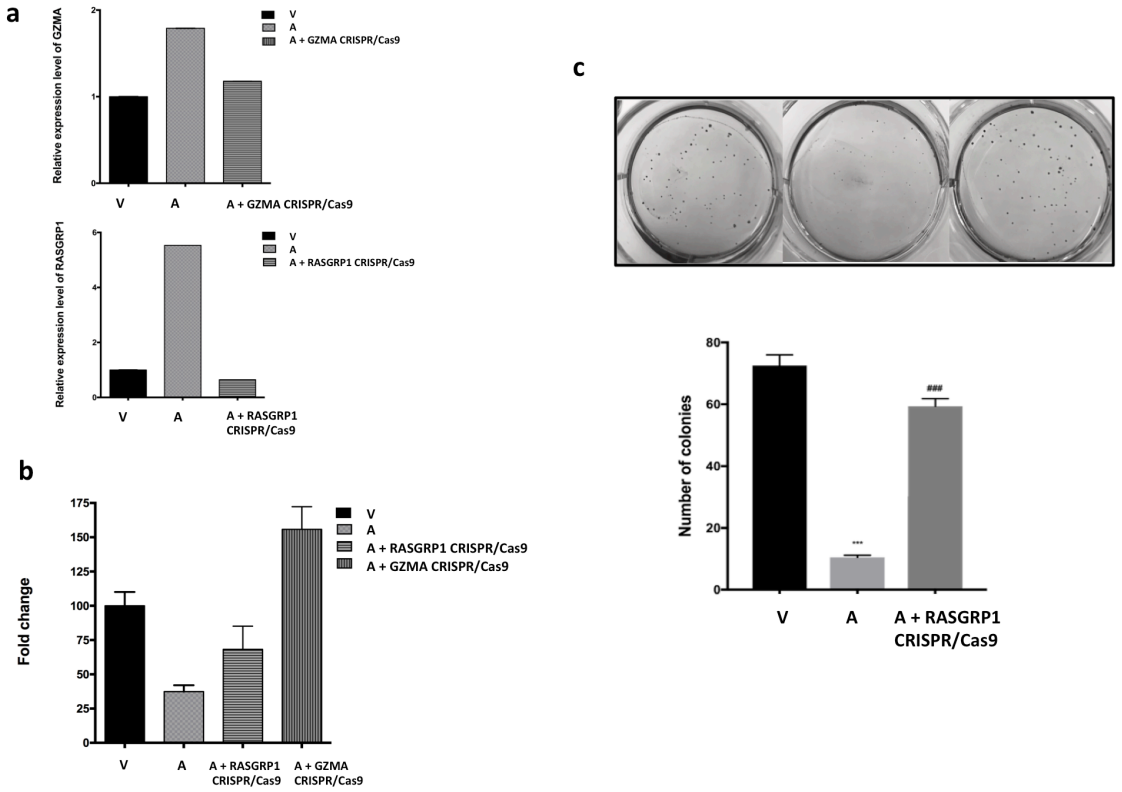

Figure 3: colony formation in soft agar. (a) qRT-PCR confirmation of *GZMA* (top panel) and *RASGRP1* (bottom panel) knockdown. b) Matrigel chamber assay showing a regain in matrigel traversal after *RASGRP1* and *GZMA* knockdown. c) Increased colony formation in soft agar following *RASGRP1* knockdown. Non-transfected virulent disseminating macrophages indicated by V and non-transfected poorly disseminating attenuated macrophages by A. Error bars represent SD. *** and ### represent $p<0.001$ compared to Virulent and Attenuated Ode macrophages, respectively.

GZMA and *RASGRP1* dampen *in vivo* dissemination of Ode macrophages

Similar to metastatic tumor cells *T. annulata*-transformed leukocytes also disseminate in immuno-deficient mice to distant organs and form proliferative foci (48). Dissemination of *Theileria*-transformed leukocytes has been previously attributed to increased production of matrix metaloproteinases (MMPs) (44, 49, 50). However, as *GZMA* and *RASGRP1* knockdown lead to a regain in matrigel traversal we used Rag2γC immunodeficient mice to test a regain in dissemination *in vivo*. The CRISPR/Cas9-induced drop in expression of

GZMA and RASGRP1 gave rise to an increase in the number of *Theileria*-containing tumors in heart, lung and mesentery, while knockdown of *RASGRP1* increased the number of tumors in the liver (Fig. 4). Thus, loss of *RASGRP1* and *GZMA* expression led to a regain in the invasive capacity of *T. annulata*-transformed macrophages into these organs.

Figure 4

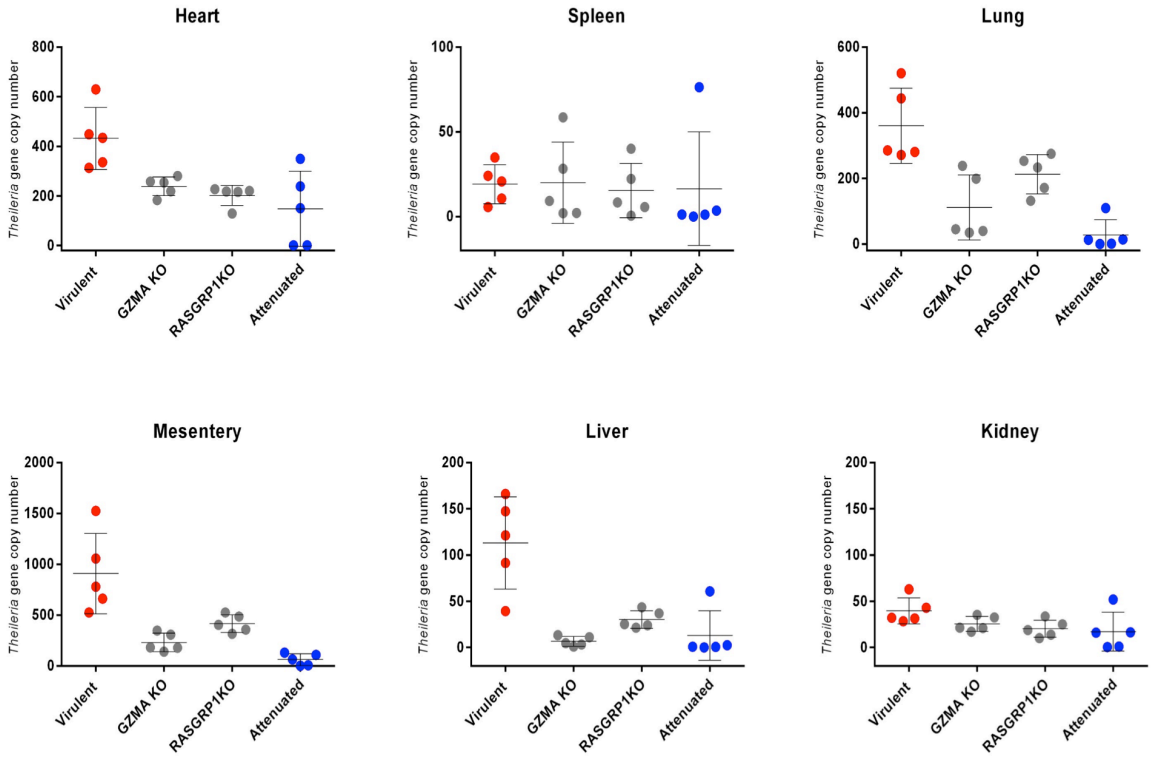

Figure 4: Effect of GZMA and RASGRP1 knockdown on transformed macrophage dissemination *in vivo.* Panels represent the copy number of the single copy *T. annulata* gene (*ama-1*, TA02980) in six internal organs: heart, lung, spleen, mesentery, left kidney and liver. Transformed macrophages were infected into five Rag2γC immunodeficient mice and plotted values represent the mean of obtained *T. annulata*-specific *ama1* gene copy number and error bars represent SD.

DISCUSSION

In this study we provide a holistic view of the transcriptional landscape of two *T. annulata*-transformed B cell lines, TBL20 and TBL3, and the virulent versus attenuated macrophage Ode vaccine line. In order to find commonly transcriptionally perturbed genes the different datasets were compared using three independent pipelines that identified four genes as potential regulators of tumor dissemination. In addition to *MMP9* we identified three other genes (*SEPP1*, *GZMA* and *RASGRP1*) as potentially having a role in dissemination. SEPP1 is a major selenoprotein involved in selenium transport and defense against oxidative stress (46). Attenuated macrophages did not survive CRISPR/Cas9-knockdown of *SEPP1* implying that death might be due to a failure to control excessive oxidative stress, since attenuated macrophages display high levels of H_2O_2 output (46). SEPP1 is downregulated in colorectal cancer and SNPs in the *SEPP1* gene are linked to increased prostate cancer and adenoma risk (51-53). Decreased SEPP1 levels induce stem cell characteristics, proliferation, oxidative stress, DNA damage, and modulation of WNT signaling (54). Given the ability of *T. annulata* infection to transform leukocytes the transcriptional down-regulation of *SEPP1* in TBL20 and TBL3 B cells correlates with the known functions of SEPP1.

RASGRP1 functions as an oncogene in many types of cancer; reviewed in (55). However, being a branch point for a diversity of signal transduction cascades that control cellular behavior, RASGRP1-activated Ras family proteins possess both pro- and anti-oncogenic properties, depending on the downstream effector pathway and cellular context; reviewed in (56). Interestingly, all members of the *RASGRP* gene family (*RASGRP1-4*) are significantly downregulated in TBL20 and TBL3, with the exception of RASGRP3 that is upregulated in TBL3. Therefore, precisely how individual RASGRPs function in *T. annulata*-transformed B cells is difficult to discern.

GZMA is a serine protease that contributes to killing tumors and pathogen-infected cells via a caspase-independent pathway (42). *GZMA*-deficient mice are more susceptible to viral (57, 58) and filarial infections (59) implying that its upregulation might be part of an anti-parasite defense mechanism by attenuated macrophages. GZMA expression induces reactive oxygen species (ROS) (60) and attenuated macrophages are known to be more oxidatively stressed than virulent macrophages (61). Indeed, H_2O_2 output was reduced in attenuated macrophages following CRISPR/Cas9-mediated *GZMA* knockdown (Fig S2).

MMP9, *SEPP1*, *RASGRP1* and *GZMA* were differentially expressed by both transformed B cells and macrophages reflecting the central role their altered expression plays in *Theileria*-induced leukocyte immortalization and dissemination. Importantly, both GZMA and RASGRP1 expression is repressed by TGF-β (62, 63), and a role for this cytokine in regulating dissemination of *Theileria*-transformed macrophages is well established (6-8). Thus, one way TGF-β promotes dissemination could be via repression of *GZMA* and *RASGRP1* transcription. As *RASGRP1*-deficient CD8 T cells exhibit markedly reduced expression of GZMB (7) the CRISPR/Cas9-mediated loss of *RASGRP1* described here could perhaps provoke a drop in *GZMA* expression rendering attenuated macrophages doubly deficient. This could underpin the more pronounced regain in dissemination that occurs upon ablating *RasGRP1* compared to *GZMA.*

Finally, GZMA can cleave APEX1 (apurinic/apyrimidinic endodeoxyribonuclease 1) after Lys31 and destroys its oxidative repair functions and APEX1 is involved in NK-cell-mediated killing via GZMA (60, 64). APEX1 prevents oxidative stress by negatively regulating Rac1/GTPase activity (65) and suppresses the activation of PARP1 during the repair of oxidative DNA damage (66). Analysis of our deep RNA-seq data revealed that *APEX1* is significantly downregulated in attenuated macrophages and taken together, it suggests that TGF-β2 by regulating a GZMA/RASGRP1/APEX1 pathway could modulate

tumor redox balance dissemination.

Acknowledgements.

This study was supported by a Competitive Research Grant from the Office for Sponsored Research (OSR-2015-CRG4-2610) at King Abdullah University of Science and Technology (KAUST) awarded to AP and GL. ZR acknowledges KAUST for awarding her PhD studentship. ST was supported by a post-doctoral fellowship from ParaFrap (ANR-11-LABX-0024) and in addition to ANR-11-LABX-0024 GL also acknowledges core support from INSERM and the CNRS. We thank members of the Bioscience Core Laboratory (BCL) at KAUST for producing the raw sequencing datasets. Franck Letourneur of the genomics platform at the Cochin institute (GENOM'IC) for quantifying the pJET-*ama-1* plasmid and Brian Shiels (University of Glasgow, Scotland) for gift of BL20/TBL20 B cells.

Author contributions.

AP and GL conceived and designed the study. ZR prepared the ssRNAseq libraries, ran and analyzed the qRT-PCR reactions. MH performed all biochemical experiments, ST the mouse *in vivo* dissemination assays, HA and ZR performed bioinformatics and data analysis. ZR and MH prepared the figures and ZR prepared the first draft of the manuscript with input from MH and FB that was then edited by GL and AP.

Supplementary figure legends

Figure S1: Sequencing quality of all samples.

(a) Clustering of all samples. (b) Density plot representing FPKM distribution of all samples. The sample names reflect the sample types and three replicates were used for each sample type.

Figure S2: Effect of *GZMA* knockdown on H_2O_2 output.

H_2O_2 levels of Vir, Att and Att Ode after CRISPR/Cas9-mediated *GZMA* knockdown. Error bars represent SD.

Table S1: Top 5 up- and down-regulated DEGs in infected and attenuated cell lines.

For details on the methods used to generate this list, please see in the Materials and Methods section.

Table S2: List of DEGs in infected and attenuated cell lines.

For details on the methods used to generate this list, please see in the Materials and Methods section.

Table S3: List of primers used for qRT-PCR

References

1. Nene V, Morrison WI. Approaches to vaccination against Theileria parva and Theileria annulata. Parasite Immunol. 2016;38(12):724-34.
2. Tretina K, Gotia HT, Mann DJ, Silva JC. Theileria-transformed bovine leukocytes have cancer hallmarks. Trends Parasitol. 2015;31(7):306-14.
3. Marsolier J, Perichon M, DeBarry JD, Villoutreix BO, Chluba J, Lopez T, et al. Theileria parasites secrete a prolyl isomerase to maintain host leukocyte transformation. Nature. 2015;520(7547):378-82.
4. Cock-Rada AM, Medjkane S, Janski N, Yousfi N, Perichon M, Chaussepied M, et al. SMYD3 promotes cancer invasion by epigenetic upregulation of the metalloproteinase MMP-9. Cancer Res. 2012;72(3):810-20.
5. Lizundia R, Chaussepied M, Huerre M, Werling D, Di Santo JP, Langsley G. c-Jun NH2-terminal kinase/c-Jun signaling promotes survival and metastasis of B lymphocytes transformed by Theileria. Cancer Res. 2006;66(12):6105-10.
6. Chaussepied M, Janski N, Baumgartner M, Lizundia R, Jensen K, Weir W, et al. TGF-b2 induction regulates invasiveness of Theileria-transformed leukocytes and disease susceptibility. PLoS Pathog. 2010;6(11):e1001197.
7. Haidar M, Whitworth J, Noe G, Liu WQ, Vidal M, Langsley G. TGF-beta2 induces Grb2 to recruit PI3-K to TGF-RII that activates JNK/AP-1-signaling and augments invasiveness of Theileria-transformed macrophages. Sci Rep. 2015;5:15688.
8. Haidar M, Echebli N, Ding Y, Kamau E, Langsley G. Transforming growth factor beta2 promotes transcription of COX2 and EP4, leading to a prostaglandin E2-driven autostimulatory loop that enhances virulence of Theileria annulata-transformed macrophages. Infect Immun. 2015;83(5):1869-80.
9. Robert McMaster W, Morrison CJ, Kobor MS. Epigenetics: A New Model for Intracellular Parasite-Host Cell Regulation. Trends Parasitol. 2016;32(7):515-21.
10. Marsolier J, Pineau S, Medjkane S, Perichon M, Yin Q, Flemington E, et al. OncomiR addiction is generated by a miR-155 feedback loop in Theileria-transformed leukocytes. PLoS Pathog. 2013;9(4):e1003222.
11. Haidar M, Rchiad Z, Ansari HR, Ben-Rached F, Tajeri S, Latre De Late P, et al. miR-126-5p by direct targeting of JNK-interacting protein-2 (JIP-2) plays a key role in Theileria-infected macrophage virulence. PLoS Pathog. 2018;14(3):e1006942.
12. Kinnaird JH, Weir W, Durrani Z, Pillai SS, Baird M, Shiels BR. A Bovine Lymphosarcoma Cell Line Infected with Theileria annulata Exhibits an Irreversible Reconfiguration of Host Cell Gene Expression. PLoS One. 2013;8(6):e66833.
13. Dobbelaere D, Heussler V. Transformation of leukocytes by Theileria parva and T. annulata. Annu Rev Microbiol. 1999;53:1-42.
14. Bierne H, Cossart P. When bacteria target the nucleus: the emerging family of nucleomodulins. Cell Microbiol. 2012;14(5):622-33.
15. Woods K, von Schubert C, Dobbelaere D. Hijacking of Host Cell Signaling by Theileria. Protein Phosphorylation in Parasites: Wiley-VCH Verlag GmbH & Co. KGaA; 2013. p. 179-98.

16. Theilen GH, Rush JD, Nelson-Rees WA, Dungworth DL, Munn RJ, Switzer JW. Bovine leukemia: establishment and morphologic characterization of continuous cell suspension culture, BL-1. J Natl Cancer Inst. 1968;40(4):737-49.
17. Morzaria SP, Roeder PL, Roberts DH, Chasey D, Drew TW. Characteristics of a continuous suspension cell line (BL20) derived from a calf with sporadic bovine leukosis. 1984.
18. Shiels BR, McDougall C, Tait A, Brown CG. Identification of infection-associated antigens in Theileria annulata transformed cells. Parasite Immunol. 1986;8(1):69-77.
19. Singh S, Khatri N, Manuja A, Sharma RD, Malhotra DV, Nichani AK. Impact of field vaccination with a Theileria annulata schizont cell culture vaccine on the epidemiology of tropical theileriosis. Vet Parasitol. 2001;101(2):91-100.
20. Bolger AM, Lohse M, Usadel B. Trimmomatic: a flexible trimmer for Illumina sequence data. Bioinformatics. 2014;30(15):2114-20.
21. Kim D, Pertea G, Trapnell C, Pimentel H, Kelley R, Salzberg SL. TopHat2: accurate alignment of transcriptomes in the presence of insertions, deletions and gene fusions. Genome Biol. 2013;14(4):R36.
22. Hardcastle TJ, Kelly KA. baySeq: empirical Bayesian methods for identifying differential expression in sequence count data. BMC bioinformatics. 2010;11:422.
23. Love MI, Huber W, Anders S. Moderated estimation of fold change and dispersion for RNA-seq data with DESeq2. Genome Biol. 2014;15(12):550.
24. Trapnell C, Hendrickson DG, Sauvageau M, Goff L, Rinn JL, Pachter L. Differential analysis of gene regulation at transcript resolution with RNA-seq. Nat Biotechnol. 2013;31(1):46-53.
25. Anders S, Pyl PT, Huber W. HTSeq--a Python framework to work with high-throughput sequencing data. Bioinformatics. 2015;31(2):166-9.
26. Livak KJ, Schmittgen TD. Analysis of relative gene expression data using real-time quantitative PCR and the 2(-Delta Delta C(T)) Method. Methods. 2001;25(4):402-8.
27. Colucci F, Soudais C, Rosmaraki E, Vanes L, Tybulewicz VL, Di Santo JP. Dissecting NK cell development using a novel alymphoid mouse model: investigating the role of the c-abl proto-oncogene in murine NK cell differentiation. J Immunol. 1999;162(5):2761-5.
28. Gotia HT, Munro JB, Knowles DP, Daubenberger CA, Bishop RP, Silva JC. Absolute Quantification of the Host-To-Parasite DNA Ratio in Theileria parva-Infected Lymphocyte Cell Lines. PLoS One. 2016;11(3):e0150401.
29. Yu Q, Stamenkovic I. Cell surface-localized matrix metalloproteinase-9 proteolytically activates TGF-beta and promotes tumor invasion and angiogenesis. Genes Dev. 2000;14(2):163-76.
30. Mangala LS, Zuzel V, Schmandt R, Leshane ES, Halder JB, Armaiz-Pena GN, et al. Therapeutic Targeting of ATP7B in Ovarian Carcinoma. Clin Cancer Res. 2009;15(11):3770-80.
31. Merlo A, Tenca C, Fais F, Battini L, Ciccone E, Grossi CE, et al. Inhibitory receptors CD85j, LAIR-1, and CD152 down-regulate immunoglobulin and cytokine production by human B lymphocytes. Clin Diagn Lab Immunol. 2005;12(6):705-12.

32. van der Vuurst de Vries AR, Clevers H, Logtenberg T, Meyaard L. Leukocyte-associated immunoglobulin-like receptor-1 (LAIR-1) is differentially expressed during human B cell differentiation and inhibits B cell receptor-mediated signaling. Eur J Immunol. 1999;29(10):3160-7.
33. Kim SO, Avraham S, Jiang S, Zagozdzon R, Fu Y, Avraham HK. Differential expression of Csk homologous kinase (CHK) in normal brain and brain tumors. Cancer. 2004;101(5):1018-27.
34. Perche PY, Vourc'h C, Konecny L, Souchier C, Robert-Nicoud M, Dimitrov S, et al. Higher concentrations of histone macroH2A in the Barr body are correlated with higher nucleosome density. Curr Biol. 2000;10(23):1531-4.
35. Kurz S, Thieme R, Amberg R, Groth M, Jahnke HG, Pieroh P, et al. The anti-tumorigenic activity of A2M-A lesson from the naked mole-rat. PLoS One. 2017;12(12):e0189514.
36. Tanaka M, Shimamura S, Kuriyama S, Maeda D, Goto A, Aiba N. SKAP2 Promotes Podosome Formation to Facilitate Tumor-Associated Macrophage Infiltration and Metastatic Progression. Cancer Res. 2016;76(2):358-69.
37. Grandclement C, Pallandre JR, Valmary Degano S, Viel E, Bouard A, Balland J, et al. Neuropilin-2 expression promotes TGF-beta1-mediated epithelial to mesenchymal transition in colorectal cancer cells. PLoS One. 2011;6(7):e20444.
38. Scott A, Wang Z. Tumour suppressor function of protein tyrosine phosphatase receptor-T. Biosci Rep. 2011;31(5):303-7.
39. Calvo A, Xiao N, Kang J, Best CJ, Leiva I, Emmert-Buck MR, et al. Alterations in gene expression profiles during prostate cancer progression: functional correlations to tumorigenicity and down-regulation of selenoprotein-P in mouse and human tumors. Cancer Res. 2002;62(18):5325-35.
40. Krzywinski M, Schein J, Birol I, Connors J, Gascoyne R, Horsman D, et al. Circos: an information aesthetic for comparative genomics. Genome Res. 2009;19(9):1639-45.
41. Burk RF, Hill KE, Awad JA, Morrow JD, Kato T, Cockell KA, et al. Pathogenesis of diquat-induced liver necrosis in selenium-deficient rats: assessment of the roles of lipid peroxidation and selenoprotein P. Hepatology. 1995;21(2):561-9.
42. Chowdhury D, Lieberman J. Death by a thousand cuts: granzyme pathways of programmed cell death. Annu Rev Immunol. 2008;26:389-420.
43. Priatel JJ, Chen X, Zenewicz LA, Shen H, Harder KW, Horwitz MS, et al. Chronic immunodeficiency in mice lacking RasGRP1 results in CD4 T cell immune activation and exhaustion. J Immunol. 2007;179(4):2143-52.
44. Baylis HA, Megson A, Hall R. Infection with Theileria annulata induces expression of matrix metalloproteinase 9 and transcription factor AP-1 in bovine leucocytes. Mol Biochem Parasitol. 1995;69(2):211-22.
45. Adamson R, Logan M, Kinnaird J, Langsley G, Hall R. Loss of matrix metalloproteinase 9 activity in Theileria annulata-attenuated cells is at the transcriptional level and is associated with differentially expressed AP-1 species. Mol Biochem Parasitol. 2000;106(1):51-61.
46. Hill KE, Dasouki M, Phillips JA, 3rd, Burk RF. Human selenoprotein P gene maps to 5q31. Genomics. 1996;36(3):550-1.

47. Short SP, Whitten-Barrett C, Williams CS. Selenoprotein P in colitis-associated carcinoma. Mol Cell Oncol. 2016;3(3):e1075094.
48. Fell AH, Preston PM, Ansell JD. Establishment of Theileria-infected bovine cell lines in scid mice. Parasite Immunol. 1990;12(3):335-9.
49. Baylis HA, Megson A, Brown CG, Wilkie GF, Hall R. Theileria annulata-infected cells produce abundant proteases whose activity is reduced by long-term cell culture. Parasitology. 1992;105 (Pt 3):417-23.
50. Somerville RP, Adamson RE, Brown CG, Hall FR. Metastasis of Theileria annulata macroschizont-infected cells in scid mice is mediated by matrix metalloproteinases. Parasitology. 1998;116 (Pt 3):223-8.
51. Al-Taie OH, Uceyler N, Eubner U, Jakob F, Mork H, Scheurlen M, et al. Expression profiling and genetic alterations of the selenoproteins GI-GPx and SePP in colorectal carcinogenesis. Nutr Cancer. 2004;48(1):6-14.
52. Cooper ML, Adami HO, Gronberg H, Wiklund F, Green FR, Rayman MP. Interaction between single nucleotide polymorphisms in selenoprotein P and mitochondrial superoxide dismutase determines prostate cancer risk. Cancer Res. 2008;68(24):10171-7.
53. Peters U, Chatterjee N, Hayes RB, Schoen RE, Wang Y, Chanock SJ, et al. Variation in the selenoenzyme genes and risk of advanced distal colorectal adenoma. Cancer Epidemiol Biomarkers Prev. 2008;17(5):1144-54.
54. Barrett CW, Reddy VK, Short SP, Motley AK, Lintel MK, Bradley AM, et al. Selenoprotein P influences colitis-induced tumorigenesis by mediating stemness and oxidative damage. J Clin Invest. 2015;125(7):2646-60.
55. Ksionda O, Limnander A, Roose JP. RasGRP Ras guanine nucleotide exchange factors in cancer. Front Biol (Beijing). 2013;8(5):508-32.
56. Cox AD, Der CJ. The dark side of Ras: regulation of apoptosis. Oncogene. 2003;22(56):8999-9006.
57. Mullbacher A, Ebnet K, Blanden RV, Hla RT, Stehle T, Museteanu C, et al. Granzyme A is critical for recovery of mice from infection with the natural cytopathic viral pathogen, ectromelia. Proc Natl Acad Sci U S A. 1996;93(12):5783-7.
58. Pereira RA, Simon MM, Simmons A. Granzyme A, a noncytolytic component of CD8(+) cell granules, restricts the spread of herpes simplex virus in the peripheral nervous systems of experimentally infected mice. J Virol. 2000;74(2):1029-32.
59. Hartmann W, Marsland BJ, Otto B, Urny J, Fleischer B, Korten S. A novel and divergent role of granzyme A and B in resistance to helminth infection. J Immunol. 2011;186(4):2472-81.
60. Martinvalet D, Zhu P, Lieberman J. Granzyme A induces caspase-independent mitochondrial damage, a required first step for apoptosis. Immunity. 2005;22(3):355-70.
61. Metheni M, Echebli N, Chaussepied M, Ransy C, Chereau C, Jensen K, et al. The level of H(2)O(2) type oxidative stress regulates virulence of Theileria-transformed leukocytes. Cell Microbiol. 2014;16(2):269-79.
62. Thomas DA, Massague J. TGF-beta directly targets cytotoxic T cell functions during tumor evasion of immune surveillance. Cancer Cell. 2005;8(5):369-80.
63. Merdrignac A, Angenard G, Allain C, Petitjean K, Bergeat D, Bellaud P, et al. A novel transforming growth factor beta-induced long noncoding RNA promotes an

inflammatory microenvironment in human intrahepatic cholangiocarcinoma. Hepatol Commun. 2018;2(3):254-69.

64. Fan Z, Beresford PJ, Zhang D, Xu Z, Novina CD, Yoshida A, et al. Cleaving the oxidative repair protein Ape1 enhances cell death mediated by granzyme A. Nat Immunol. 2003;4(2):145-53.

65. Ozaki M, Suzuki S, Irani K. Redox factor-1/APE suppresses oxidative stress by inhibiting the rac1 GTPase. FASEB J. 2002;16(8):889-90.

66. Peddi SR, Chattopadhyay R, Naidu CV, Izumi T. The human apurinic/apyrimidinic endonuclease-1 suppresses activation of poly(adp-ribose) polymerase-1 induced by DNA single strand breaks. Toxicology. 2006;224(1-2):44-55.